

# Size analysis of single fullerene molecules by electron microscopy

Anish Goel<sup>a,\*</sup>, Jack B. Howard<sup>a,\*</sup>, John B. Vander Sande<sup>b</sup>

<sup>a</sup> Department of Chemical Engineering, Massachusetts Institute of Technology, 77 Massachusetts Avenue, Cambridge, MA 02139-4307, USA

<sup>b</sup> Department of Materials Science and Engineering, Massachusetts Institute of Technology 77 Massachusetts Avenue, Cambridge, MA 02139-4307, USA

Received 8 August 2003; accepted 10 March 2004

Available online 24 April 2004

## Abstract

Individual fullerene molecules were observed and sized using high resolution transmission electron microscopy. Fullerene C<sub>60</sub> molecules were tethered by chemical bonding to carbon black particles to facilitate HRTEM imaging and sizing of known fullerenes. HRTEM analysis of soot samples from a fullerene-forming flame revealed the presence of a range of fullerenes from C<sub>36</sub> to C<sub>176</sub> and larger fullerene-like structures. The observation of fullerenes smaller than C<sub>60</sub> is noteworthy in that such structures necessarily contain adjacent pentagons and hence are strained and expected to have interesting reactivity that may be useful in certain applications. HRTEM can be used to detect and size fullerenes in samples containing fullerenes but not in sufficient quantity, or not sufficiently removable, to be detectable by chemical analysis.

© 2004 Elsevier Ltd. All rights reserved.

**Keywords:** A. Carbon black, Fullerene, Soot; C. Electron microscopy; D. Microstructure

## 1. Introduction

An ability to observe and measure the size of an individual fullerene molecule by high resolution transmission electron microscopy (HRTEM) is of interest for several reasons. Such a technique would offer a possible means for extending the detection and analysis of fullerenes to lower limits of detection than can be attained by conventional chemical analysis. For example, circular objects approximately the size of C<sub>60</sub> and C<sub>70</sub> fullerenes can be seen in HRTEM images of soot not only from certain low-pressure benzene/oxygen flames well known to contain fullerenes but also from atmospheric-pressure ethylene/air flames in which fullerenes could not be detected by state-of-the-art chemical analysis [1].

The HRTEM technique would be useful also for the detection and characterization of fullerenes which are too strongly bound to, or within, the material with which they are condensed in the synthesis process to

permit easy removal for chemical analysis. Such species include fullerenes smaller than C<sub>60</sub>, all of which necessarily contain adjacent pentagons in their structure and are strongly curved and strained, and hence interactive, and much larger fullerenes whose size facilitates extensive contact and increases the opportunity for bonding interactions. Curved carbon structures seen in HRTEM images of soot from fullerene-forming flames exhibit radii of curvature which include not only values comparable to those of the prevalent fullerenes C<sub>60</sub> and C<sub>70</sub> but also smaller and larger values [1–3]. Carbon structures with radii of curvature less than that of C<sub>60</sub> may be indicative of adjacent pentagons, the presence of which in carbon layers would be of sufficient practical and scientific interest to merit confirmation and further study by more quantitative HRTEM analysis.

Mass spectra which show the presence of C<sub>60</sub>, C<sub>70</sub> and higher fullerenes in the vapor from graphite vaporization [4] and in low-pressure flames of certain hydrocarbons [5] also exhibit mass peaks corresponding to C<sub>50</sub> and other carbon species lighter than C<sub>60</sub>. Under some flame conditions the apparent abundance of C<sub>50</sub> is even comparable to that of C<sub>60</sub> and C<sub>70</sub> [5,6]. However, C<sub>50</sub> fullerene has never been found in chemical analysis of condensed material from fullerene-containing flames or carbon vaporization systems, possibly reflecting the

\* Corresponding authors. Tel.: +1-202-736-4256; fax: +1-202-736-4259 (A. Goel), Tel.: +1-617-253-4574; fax: +1-617-324-0066 (J.B. Howard).

E-mail addresses: [anish@mit.edu](mailto:anish@mit.edu) (A. Goel), [jbhoward@mit.edu](mailto:jbhoward@mit.edu) (J.B. Howard).

difficulty of extracting this compound from the soot and other components of the condensate. The structure of  $C_{50}$  is expected to contain five pairs of adjacent pentagons and hence to be highly strained and strongly attracted to the other molecules, including  $C_{50}$ , and surfaces in the condensed material. Fullerene  $C_{36}$  which, even more than  $C_{50}$ , is highly strained and prone to forming strong bonds with the condensed material, has been identified in material condensed from a fullerene-forming graphite vaporization process using fractionation and analysis methods especially designed to deal with the strong bonding [7]. The smallest possible fullerene,  $C_{20}$ , consisting solely of 12 pentagons, has been generated from a brominated hydrocarbon, dodecahedrane, by gas-phase debromination [8]. The lifetime of the  $C_{20}$  cage under the experimental conditions used was at least 0.4 ms. Owing to the extreme curvature and reactivity of this structure, it would not be expected to attain substantial gas-phase concentrations in most methods of fullerene synthesis. Nevertheless, it is conceivable that the  $C_{20}$  cage might be stabilized for longer lifetimes through strong bonding with soot or other condensed species. A HRTEM capability to observe directly in the condensed phase  $C_{50}$ ,  $C_{36}$ ,  $C_{20}$  and other highly interactive fullerenes, both smaller and much larger than  $C_{60}$ , and to contribute to their characterization would clearly be useful.

The observation of single fullerene molecules by HRTEM has been addressed previously. Cox et al. [9] deposited  $C_{60}$  on MgO crystals supported on holey carbon films. Circular contrast patterns with about 0.8 nm diameter, consistent with that of  $C_{60}$ , were observed on the MgO crystals and could be seen most clearly on the edges of crystals hanging over holes in the support film. The circular images were not seen on MgO crystals without  $C_{60}$  deposition. Cox et al. [9] regarded it to be improbable that the circular patterns could represent two or more  $C_{60}$  molecules aligned parallel to the electron beam axis. The strong inference is that the observed circular patterns were images of individual  $C_{60}$  cages. Ajayan and Iijima [10] observed with HRTEM a 0.8 nm diameter circular image at the outside edge of the image of a multilayer truncated conical carbon nanostructure. The authors point out that the image could correspond to a single  $C_{60}$  structure but they argue against such an interpretation on the grounds that the contrast exhibited by the small circular image is comparable to that of the lattice fringes of the much larger supported multilayered structure. Instead, they interpret the circular image to be an end-on view of a nanotube having the same diameter as a  $C_{60}$  molecule and a length of a few such units in the direction perpendicular to the plane of the image. Saito et al. [11] present a HRTEM image of a round, hollow single-layered particle of 1.3 nm diameter, which they suggest may be a fullerene having approximately 200 carbon atoms, held by a single-walled carbon nanotube

of approximately the same diameter. Based on this observation the authors suggest it should be possible, although they had not been able yet, to observe by TEM more prevalent fullerenes such as  $C_{60}$ ,  $C_{70}$ , and  $C_{84}$  suspended on the tip or side of a carbon nanotube.

Fuller and Banhart [12] using HRTEM observed not only fullerene cages but also the formation of the cages during electron irradiation of carbon specimens in the electron microscope. They observed tube-like structures as well as spherical cages, and saw that tube-like structures viewed end-on resembled, but gave much more contrast than, spherical cages. In a HRTEM study of fullerene nanostructures from fullerene producing flames, Das Chowdhury et al. [13] observed on a multiwalled carbon nanotube an ellipsoidal structure having a single closed-shell whose major and minor diameters were about 1.1 and 0.7 nm, corresponding approximately to a  $C_{94}$  fullerene molecule.  $C_{94}$  fullerene has been isolated since and identified by solvent extraction and HPLC analysis of condensable material collected from flames [14]. Burden and Hutchison [15] using HRTEM observed features consistent with fullerenes  $C_{60}$  and  $C_{70}$  on the surface of carbon black particles irradiated with an electron beam in the presence of helium. Smith et al. [16] and Sloan et al. [17] obtained HRTEM images of round, closed shells of carbon, apparently fullerenes, encapsulated within the hollow central region of individual single-wall carbon nanotubes produced in carbon vaporization systems. The diameters of the apparent fullerenes correspond to  $C_{60}$  [16,17] and various other fullerenes both smaller and larger than  $C_{60}$ , ranging from 0.4 to 1.6 nm [17]. The estimated precision in the diameter measurements of Sloan et al. [17] was  $\pm 0.05$  nm.

Although previous studies (mentioned above) provide strong evidence that individual fullerene molecules can be observed using HRTEM, such capability has been questioned [10]. There is need for unequivocal demonstration of the capability of HRTEM for observing and sizing fullerene molecules on or within condensed carbon material in order to establish the viability of the technique for use in the detection and characterization of fullerenes which are below the detection limit, or are difficult to transfer to the gas or liquid phase, for chemical analysis. Furthermore, there is need to apply the capability, once it is established, to the study of bound fullerenes in combustion-generated material, which could be produced in whatever large quantities might eventually be demanded by practical applications. To these ends, the present study (1) tests the capability of HRTEM for observing individual  $C_{60}$  fullerene molecules added in a controlled manner to a sample of carbon material, (2) calibrates the HRTEM measurement of fullerene diameters against a known standard, and (3) uses the established HRTEM technique to identify and size interesting flame-generated fullerenes

that cannot be removed easily from the other condensed material for conventional chemical analysis.

## 2. Experimental

Three different samples were prepared for investigation by HRTEM. The first sample was pure carbon black (Regal 330; Cabot Corp.) suspended in a toluene solution. The other two samples were prepared from a portion of the carbon black–toluene solution to which was added a specified amount of dichloromethano[60]fullerene (obtained from Professor Mark S. Meier, the University of Kentucky). In this functionalized fullerene, the carbon atom of the functional group is bridged to two carbon atoms of the fullerene molecule. It was expected, based on known behavior of the similar dibromomethano[60]fullerene [18], that the two chlorine atoms could be substituted readily to provide a chemical tether to a compound of interest. After a uniform dispersion was ensured with vigorous mixing, the toluene was allowed to evaporate and the resulting dry powder mixture was sealed inside an argon-filled glass tube. The entire unit was then heat treated at approximately 400 °C for 4.5 h in a tubular furnace (Lindberg Model 55036) and then cooled. The material was removed from the tube and divided into two parts. One of these two samples was not treated further and hence consisted of carbon black with tethered fullerenes and any fullerenes that remained untethered. This sample is referred to as pre-extraction. The other of these two samples was extracted by sonication in toluene for 13 min followed by vacuum filtration with a 0.45- $\mu\text{m}$  nylon filter to remove any untethered fullerenes. Thus, this sample, referred to as post-extraction, consisted of carbon black with only tethered fullerenes.

A diluted suspension of each of the three samples in toluene was deposited onto a lacey carbon grid and the toluene was allowed to evaporate. The samples were analyzed in a JEOL 2010 electron microscope operating at 200 kV. The images obtained were analyzed for the presence of fullerene-type structures, i.e., structures that appear to be completely closed cages. In each image, the number of fullerene-type structures per length of perimeter, referred to as linear concentration, was deter-

mined and the diameter of each of those structures was measured. The data then were aggregated across all the images of a particular sample to provide fullerene linear concentration data and fullerene size distribution data.

Additional HRTEM analyses were performed on soot material collected from a pre-mixed benzene/oxygen/argon flame that has been extensively characterized and studied previously [1,19]. The conditions of this flame are: pressure, 40 Torr; gas velocity at burner, 25 cm/s (25 °C); fuel equivalence ratio, 2.4 (atomic C/O ratio, 0.96); and percentage diluent in feed gas, 10% argon. Samples of soot and all other condensables from this flame were collected in the manner described previously [1] and HRTEM analysis was done using the same JEOL 2010 operating at 200 kV. Gold islands were deposited on the surface of several of these samples to provide a magnification calibration for the HRTEM images. Gold has a stable planar structure with a constant interplanar spacing of 2.039 Å for the {111} atomic planes. By observing and measuring this known spacing in an image, the image length scale thus is calibrated allowing the dimensions of other structures to be accurately measured. This calibration was used to measure the sizes of several of the closed-cage structures that were observed in the images and the data were compiled across all of the samples into a size distribution histogram.

Three influences on the accuracy of the electron microscopy observations have been considered in this work. First, the influence of the degree of objective lens defocus (measured in nm with negative numbers being underfocus and positive numbers being overfocus) has been investigated. Calculations [20] were performed on  $\text{C}_{60}$  using 200 kV electrons, a spherical aberration coefficient of 0.5 mm, an incident beam spread of 4 nm over a defocus range of  $-35$  to  $+35$  nm in 5 nm intervals. One result from such calculations is shown in Fig. 1. Note that the only interpretable images are at an underfocus of  $\sim -30$  nm yielding an image consisting of a very dark “doughnut” surrounded by a “halo”. The variation in measured size (using the interface between the “doughnut” and the “halo”) is  $\pm 0.02$  nm in the underfocus range of  $-30 \pm 5$  nm.

The second source of inaccuracy pursued was that associated with the practical obtaining of images, i.e.,

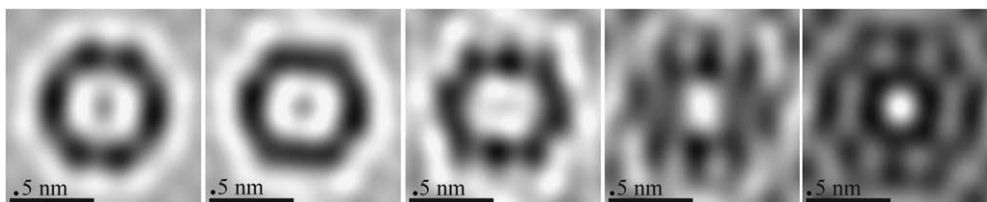


Fig. 1. A series of simulated electron microscope images of  $\text{C}_{60}$  viewed in the [1 0 0] direction. This sequence consists of images over an objective lens defocus of  $-35$  nm (left-most image) to  $-15$  nm (right-most image), bracketing the defocus where interpretable images are produced. The  $\text{C}_{60}$  image consists of a dark “doughnut” surrounded by a bright “halo”. See text for additional information.

the experimental work. Fig. 2 shows a series of images taken from the same area. The black dashes in Fig. 2 indicate a structure indicative of those measured in this analysis. The variation of diameters measured is a convolution of objective lens defocus and changes in the object over the time associated with sample radiation and heating. Observation of images such as those in Fig. 2 lead to the establishment of the accuracy of observations of  $\pm 0.05$  nm.

Third, the use of the gold islands as a magnification calibration leads to a measurement precision of  $\pm 0.01$  nm. It is clear that the practical aspects of performing the electron microscopy, as embodied in Fig. 2, limit the accuracy of observations in this work to  $\pm 0.05$  nm.

Finally, a sample of  $C_{60}$  molecules (99.5% pure; SES Corporation) was examined under HRTEM. The fullerenes were dissolved into toluene and drops of the solution were placed on TEM grids. The toluene was allowed to evaporate before the HRTEM analysis.

### 3. Results

Figs. 3 and 4 show two images that are representative of the images analyzed from the different carbon black samples. Fig. 3 is an image of a particle taken from pure carbon black while Fig. 4 shows a particle from the post-extraction sample.

The black dashes in Fig. 4 are observer-added indications of structures that were deemed to be fullerene and included in the concentration and size data. Note that the contrast from the fullerenes in Fig. 4 are qualitatively similar to the calculated images shown in Fig. 1. The absence of black dashes in Fig. 3 highlights the lack of fullerene-type structures in the carbon black sample. Only carbon structures along the periphery of the particles were analyzed as only the periphery was thin enough to allow for observation and accurate measurements of the structures [2]. The hand-drawn black line in the inset to Fig. 4 shows the boundary between the area that was analyzed and the particle interior, whose thickness presents too many stacked

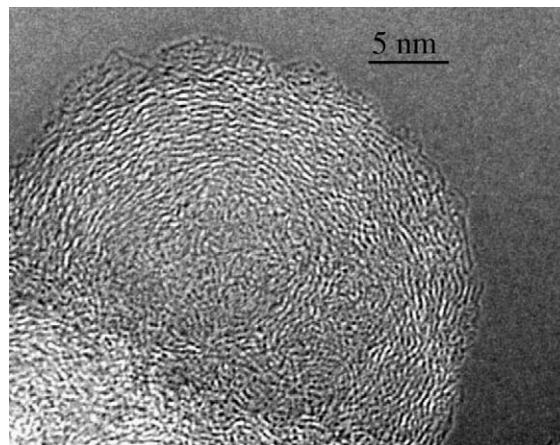


Fig. 3. HRTEM image of a particle from a pure carbon black sample.

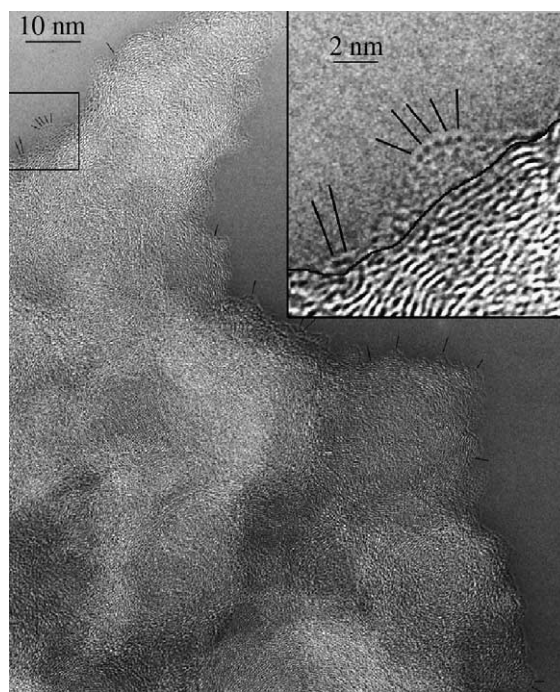


Fig. 4. HRTEM image of a particle from post-extraction tethered fullerene sample.

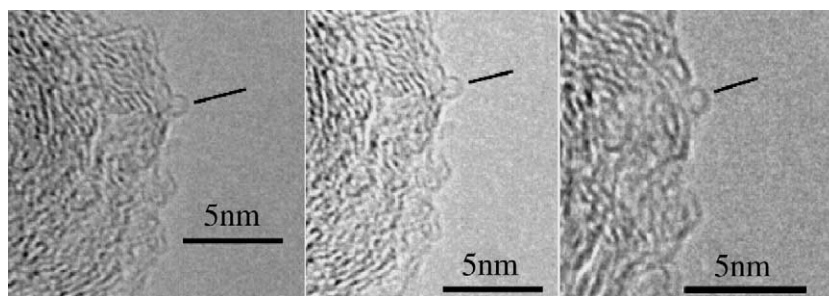


Fig. 2. A series of three electron microscope images, taken of the same area of a combustion generated fullerene sample, over a short time span. The degree of objective lens defocus (in the range of  $-30$  nm) is also varying amongst the images. A  $C_{60}$ -like molecule can be seen in each image, the measured size of which varies.

carbon layers to allow for accurate structural identification. It is unclear whether perceived structures in the particle interior inside the boundary are in fact single structures or the result of superpositioning of two or more different structures. Only the material outside the boundary was sufficiently thin to ensure interpretable observations. Qualitatively, the images show quite clearly that the carbon black doped with tethered fullerenes has many more fullerene-type structures than the pure carbon black particles.

Quantitative analyses of the same images reinforces the qualitative observation. Fig. 5 shows the method used to perform the quantitative analyses. It can be seen from this cartoon, corresponding to the five condensed structures in the inset to Fig. 4, that both vertical and horizontal height (diameter) were measured and then averaged. This averaged diameter was then used for size distribution purposes. Table 1 gives a summary of the fullerene concentration data.

From Table 1, it is seen that both samples containing tethered fullerenes have a fullerene concentration almost an order of magnitude greater than the concentration of what appears to be fullerenes in the pure carbon black sample. It should be noted that the post-extraction sample does have a slightly lower concentration than the pre-extraction samples. This is not surprising as it is expected that less than 100% of the functionalized fullerenes would react with the carbon black, leaving

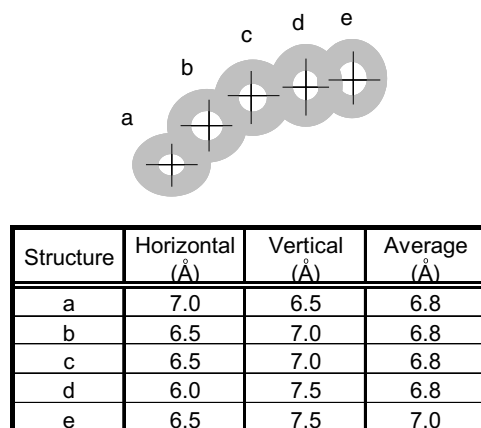


Fig. 5. Measurement method used for structure diameter size distribution.

some untethered fullerenes to be separated during extraction.

It should be noted also that both the pre- and post-extraction samples exhibit concentrations less than what would correspond to the total amount of functionalized fullerenes added in the experiment. Considering the relative amounts of carbon black and functionalized fullerenes utilized, and assuming a uniform distribution of fullerenes over the superficial surface of the carbon black, the calculated area concentration of fullerene molecules would be 0.25 molecules/nm<sup>2</sup>. The corresponding linear concentration of fullerenes would be 0.50 molecules/nm. Both tethered samples yield a linear concentration approximately 20% of this theoretical value indicating that many of the fullerenes are not observed. This result is not surprising given the difficulty of finding and observing fullerenes on the carbon black particles (see next section).

Figs. 6–8 show representative images taken from the analysis of samples of flame-generated soot. The striped patterns in Fig. 6 are the lattice fringe images of the {111} planes from the deposits of gold that were used to calibrate the microscope. Figs. 7 and 8 show other areas of the soot and several key structures are indicated by the arrows. The numbers associated with the highlighted structures are the observed diameters using the gold calibration as identified in Fig. 6. It can be seen

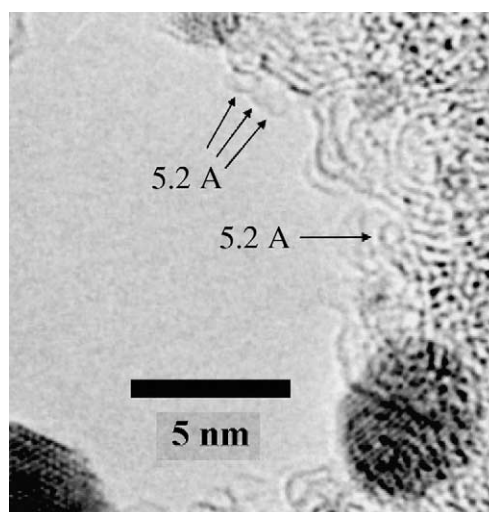


Fig. 6. HRTEM image of flame soot with gold island deposits and showing structures smaller than C<sub>60</sub>.

Table 1

Linear concentration analysis of C<sub>60</sub> fullerene-like structures in HRTEM images of carbon black with and without tethered C<sub>60</sub> fullerene molecules

Sample number and description	No. of fullerenic structures	Perimeter length (nm)	Fullerenic structures per 1000 nm of perimeter
1. Without tethered C <sub>60</sub>	21	1775	12
2. With tethered C <sub>60</sub> ; pre-extraction	209	2220	94
3. With tethered C <sub>60</sub> ; post-extraction	172	1970	87

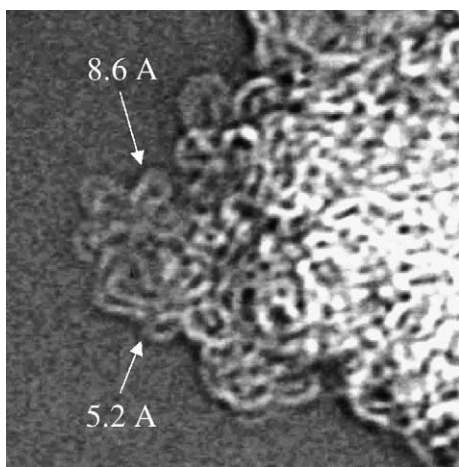


Fig. 7. HRTEM image of flame soot showing structures both larger and smaller than  $C_{60}$ .

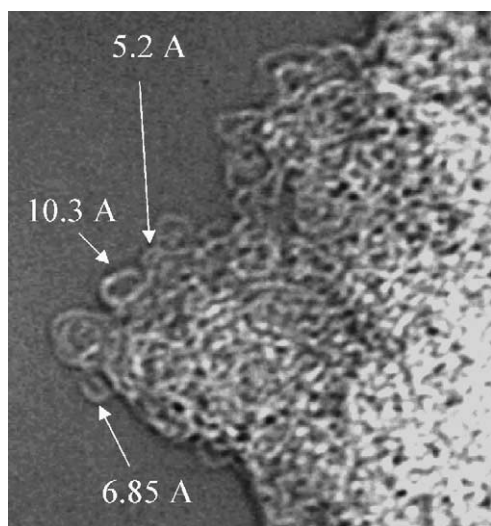


Fig. 8. HRTEM image of flame soot showing structures larger than, smaller than, and the size of,  $C_{60}$ .

from the indicated structures in Figs. 6–8 that not only are structures the size of  $C_{60}$  and larger observed (structures marked 6.85, 8.6, and 10.3 Å), but those smaller than  $C_{60}$  are prevalent as well (structures marked 5.2 Å).

The size-distribution histogram obtained from the measurement of these structures is seen in Fig. 9. The size is an average of the major and minor axes of these, generally non-round structures. In the histogram, the numbers along the  $x$ -axis represent the bins that were used to separate out the measurements. The arbitrary nature of the bin sizes and cut-offs is a consequence of the resolution limit of the measurement technique. It can be seen from Fig. 9 that there is a significant peak in the bin containing 7 Å, which is the diameter of  $C_{60}$ . In addition, Fig. 9 shows that structures of average dimension both larger *and* smaller than  $C_{60}$  are prevalent in the samples. This indicates that we are in fact observing and identifying structures that are not only larger than  $C_{60}$  but smaller as well. The implications of these observations are discussed in greater detail in the next section.

Fig. 10 shows a representative HRTEM image from the analysis of  $C_{60}$  precipitated from solution directly onto the TEM grid. The  $C_{60}$  molecules have taken a crystalline form with a twofold symmetry that is visible. Comparing the length scale to the black centers of the individual molecules reveals a diameter of about 0.7 nm as expected for  $C_{60}$  molecules. The measured center-to-center distance between the molecules is 1.01 nm along two of the crystallographic directions and 1.14 nm along the third direction.

#### 4. Discussion

A previous study by Hebgen et al. [2] reported what appear to be structures smaller than  $C_{60}$ . Diameter histograms from that study show a significant number of

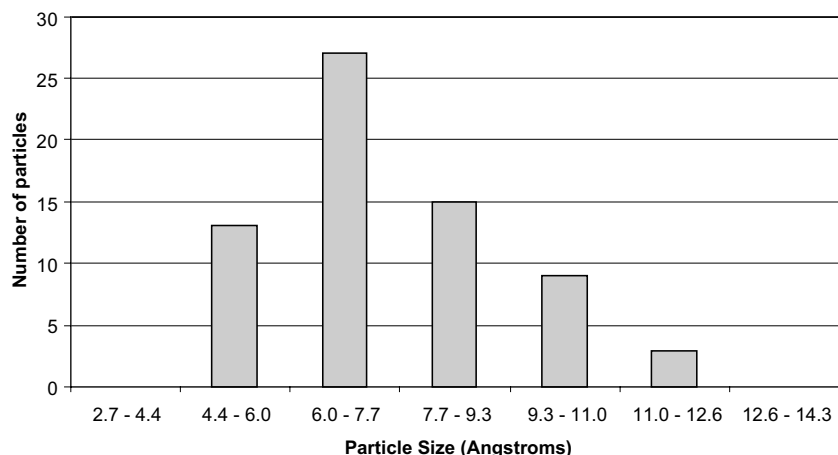


Fig. 9. Size distribution histogram of structures measured in HRTEM images of flame-generated soot.

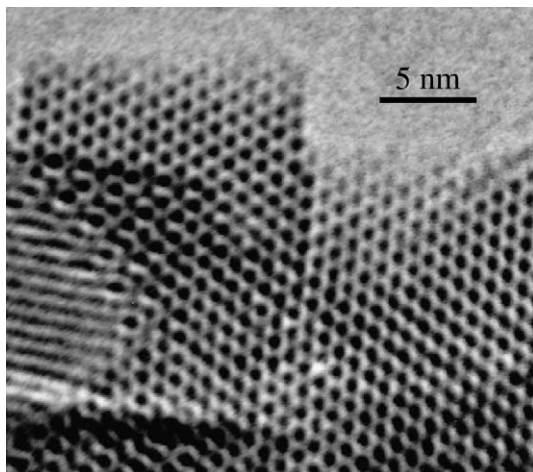


Fig. 10. HRTEM image of a pure  $C_{60}$  sample.

structures with diameters less than  $7 \text{ \AA}$ . The possible existence of small fullerenes is strengthened by the observation that the peak of the diameter distribution shifts from  $5$  to  $7 \text{ \AA}$  and back again with increasing residence time, indicating that the smaller structures are not an artifact of the measurement method. However, the data in the previous study [2] may be inconclusive because of user error in the MATLAB measurement method. This error results from inaccuracies in placing the user-defined marks exactly on the structures in the MATLAB program. Although the marks generally are accurate, misplacing them by one or two pixels, which is not uncommon, can result in significant error in the diameter measurements, especially for small structures, since MATLAB calculates the diameter based on the locations of the user-defined marks. This error has been estimated at  $\sim \pm 1.5 \text{ \AA}$  for all structures or up to 35% for structures in the  $5\text{--}6 \text{ \AA}$  range. This error limits the conclusiveness of the observation of structures smaller than  $C_{60}$  by Hebgren et al. [2]. Fortunately, other factors strengthen the data. Any error inherent in the method would be averaged out by the immense amount of data taken and the shift in peak location would indicate that the structures in general are smaller in one sample than another. In addition, the error was found to have a slightly positive bias meaning that structures tend to be measured larger than they actually are. This suggests that some of the small structures are actually smaller than indicated. Given this overall ambiguity, though, the Hebgren et al. [2] data call for more conclusive measurements, which the present study provides. The HRTEM images of known fullerene molecules prove that these fullerenes and probably those of other sizes can be seen by HRTEM and verify the method used by Hebgren et al. [2].

The above-mentioned previous observation [9] of  $C_{60}$  on MgO crystals was in an experimental situation similar to that used in the present work. Given this prece-

dent and the data presented above, we believe that the contrast observed, for instance in Fig. 4, is consistent with single  $C_{60}$  molecules. It should be noted that the contrast in Fig. 4 is exactly analogous to that in Fig. 10, which is known to show  $C_{60}$  molecules. The order of magnitude increase in observed fullerenic-type structures in doped-with- $C_{60}$  samples strengthens the conclusion that  $C_{60}$  molecules are being observed. This coupled with the qualitative observations indicates quite strongly that fullerenes have been tethered to the carbon black surface, and furthermore, that these fullerenes are observable with HRTEM.

Nonetheless, precautions must be taken to reduce the influence of radiation damage and/or beam heating on the observations. Such influences include degradation of the sample, incorporation of smaller structures into larger ones, and migration of molecules. All three of these scenarios have been observed during HRTEM imaging and all can contribute to an artificially low frequency of fullerene observations. For example, we have observed  $C_{60}$ , and other fullerenic molecules, migrating “behind” the carbon black under some observation conditions, in accord with earlier reports [12].

While care is taken to minimize the effects of these imaging artifacts, some error will still be incorporated into the imaging results. This reduction in fullerenic structure observations gives a plausible explanation as to why, as mentioned in the previous section, the observations account for only 20% of the expected theoretical value. Normally, a 20% agreement would be cause for concern but given the fact that we observe still an order-of-magnitude increase in fullerenic structures with tethered fullerenes, the conclusions are not weakened.

To stem any lingering uncertainties about the measurement method used in the tethered fullerene experiment and to accurately measure structures smaller than  $C_{60}$ , the gold island calibration method was developed and used to analyze images of flame-generated soot. The high precision and accuracy of this method give it a significant advantage over both the measurement method from Hebgren et al. [2] and the method used in the tethered fullerene experiment above. The observation of structures smaller than  $C_{60}$  in the experiments using gold calibration (Figs. 6–9) proves conclusively that such small structures do exist and that they are not artifacts of the method. The measured diameters range from about  $0.5$  to about  $1.2 \text{ nm}$  (see Fig. 9). As stated in Section 2 of this paper, an accuracy of  $\pm 0.05 \text{ nm}$  has been demonstrated for these observations. A simple calculation using  $0.7 \text{ nm}$  as the diameter of  $C_{60}$  and approximating all fullerene molecules as spherical shells whose mass is proportional to the square of the diameter gives  $0.5 \text{ nm}$  as the diameter of  $C_{36}$  and  $1.2 \text{ nm}$  as the diameter of  $C_{176}$ . The diameter of  $C_{36}$  as represented by

the carbon center to carbon center distance has been reported to be 0.5 nm [21–23]. Average diameters of selected structures marked for illustration in Figs. 6–8 include 0.52, 0.685, 0.86, and 1.03 nm, corresponding to  $C_{36}$ ,  $C_{58}$ ,  $C_{90}$  and  $C_{130}$ . Many other closed-cage structures with sizes corresponding to  $C_{50}$  and other fullerenes were also observed, as were fullerene-like structures much larger than the  $C_{176}$  mentioned above.

These conclusions from the present study lend credence to the data from the Hebggen et al. study [2]. The observation of closed-cage structures, apparently fullerenes, both smaller and larger than  $C_{60}$  has been confirmed and the error in the measurement method used in that study is not significant enough to alter its results. This has major implications for the MATLAB method of measuring structures that was utilized. It seems that the method is accurate and can be used to positively identify structures both similar to  $C_{60}$  and smaller and to characterize structures in fullerene soots including curvatures and sizes. Additionally, it can be seen that this technique is much more sensitive than chemical analysis as fullerenes can be “observed” in samples from which sufficient quantities of fullerenes could not be vaporized or dissolved to reach or exceed the detection limit of chemical analysis methods. Thus HRTEM can reveal the presence of fullerenes in soot material otherwise thought to contain none [1].

The confirmed existence of sub- $C_{60}$  fullerenes also indicates the presence of adjacent carbon pentagon rings in these fullerenes, which has important implications for bulk soot properties. Adjacent pentagons result in unique structural and electrical properties in the soot that can be exploited for the development of commercially useful products. Additionally, sub- $C_{60}$  molecules indicate the possible existence of single-walled carbon nanotubes with diameters smaller than  $C_{60}$ , which have been suggested but not confirmed outside of a support matrix.

## 5. Conclusions

High resolution transmission electron microscopy (HRTEM) was used in this study to obtain images of individual fullerene molecules that reveal the shape and size of the molecules. The molecular diameter could be specified and measured to within  $\pm 0.05$  nm.

A method was developed for tethering fullerene molecules by chemical bonding to a carbon surface. Through chemical tethering of test molecules to a surface and subsequent HRTEM analysis, known fullerene molecules were successfully observed and sized, thus confirming the efficacy of the method.

Use of the HRTEM method in the analysis of soot and associated condensables collected from a fullerene-forming flame revealed the presence of closed-cage car-

bon structures having the appearance of fullerene molecules ranging in diameter from about 0.5 nm, corresponding to  $C_{36}$ , to 1.2 nm, corresponding to  $C_{176}$ . Larger fullerene-like structures were also present. Previous chemical analysis of samples from the same flame shows the presence of numerous fullerenes ranging from  $C_{60}$  to  $C_{116}$  and lends credence to the assumption that the closed-cage structures seen in the HRTEM images are indeed fullerene molecules.

The observation of fullerenes smaller than  $C_{60}$ , such as  $C_{36}$  and  $C_{50}$ , is noteworthy since such structures necessarily contain some number of paired or adjacent pentagons. The increased strain and reactivity of these small fullerenes, which render them difficult to remove from the soot and other condensables with which they are collected, may give them interesting properties for certain applications.

The HRTEM method demonstrated in this study offers a means for the detection and characterization of fullerenes in samples from which the amount of fullerenes that can be vaporized or dissolved in a liquid for chemical analysis is below the detection limit of conventional analytical methods.

## Acknowledgements

We are grateful to Professor Mark S. Meier and Mr. Mathew M. Meyer, University of Kentucky for preparation of the functionalized fullerenes, to Mr. Murray J. Height, MIT, for sample synthesis, to Drs. Paula Jardim, Paulo Ferreira, and K. Das Chowdhury, MIT, for HRTEM work, and Mr. Jin Ho An, University of Texas, for image simulations. Different parts of the work described here were supported by the Division of Materials Science (Grant No. DE-FG02-85ER 45179) and the Division of Chemical Sciences (Grant No. DE-FG02-84ER 13282), Office of Basic Energy Sciences, Office of Energy Research, United States Department of Energy.

## References

- [1] Grieco WJ, Howard JB, Rainey LC, Vander Sande JB. Carbon 2000;38:597–614.
- [2] Hebggen P, Goel A, Howard JB, Rainey LC, Vander Sande JB. Proc Combust Inst 2000;28:1397–404.
- [3] Goel A, Hebggen P, Vander Sande JB, Howard JB. Carbon 2002;40:177–82.
- [4] Rohlffing EA, Cox DM, Kaldor A. J Chem Phys 1984;81:3322–30.
- [5] Gerhardt P, Loffler S, Homann KH. Chem Phys Lett 1987;137:306–9.
- [6] Baum T, Loffler S, Loffler P, Weilmunster P, Homann KH. Ber Bunsen Phys Chem 1992;96:841–57.
- [7] Piskoti C, Yarger J, Zettl A. Nature 1998;393:771–4.
- [8] Prinzbach H, Weller A, Landenberger P, Wahl F, Worth J, Scott LT, et al. Nature 2000;407:60–3.



- [9] Cox DM, Behal S, Disko M, Gorun SM, Greaney M, Hsu CS, et al. *J Am Chem Soc* 1991;113:2940–4.
- [10] Ajayan PM, Iijima S. *Nature* 1992;358:23.
- [11] Saito Y, Yoshikawa T, Mitsumasa O, Naoya F, Sumiyama K, Suzuki K, et al. *J Phys Chem Solids* 1993;54:1849–60.
- [12] Fuller T, Banhart F. *Chem Phys Lett* 1996;254:372–8.
- [13] Das Chowdhury K, Howard JB, Vander Sande JB. *J Mater Res* 1996;11:341–7.
- [14] Richter H, Labrocca AJ, Grieco WJ, Taghizadeh K, Lafleur AL, Howard JB. *J Phys Chem B* 1997;101:1556–60.
- [15] Burden AP, Hutchison JL. *Carbon* 1998;36:1167–73.
- [16] Smith B, Monthieux M, Luzzi DE. *Chem Phys Lett* 1999;315: 31–6.
- [17] Sloan J, Dunin-Borkowski RE, Hutchison JL, Coleman KS, Williams VC, Claridge JB, et al. *Chem Phys Lett* 2000;316:191–8.
- [18] Meier MS. Department of Chemistry, University of Kentucky, Personal communication, 2001.
- [19] Grieco WJ, Lafleur AL, Swallow KC, Richter H, Taghizadeh K, Howard JB. *Proc Combust Inst* 1998;27:1669–75.
- [20] SimulaTEM, Beltran de Rio L, editor. 1.1. Mexico: UNAM; 1998.
- [21] Cote M, Grossman JC, Louie SG, Cohen ML. *Bull Am Phys Soc* 1997;42:270.
- [22] Grossman JC, Cote M, Louie SG, Cohen ML. *Bull Am Phys Soc* 1997;42:1576.
- [23] Grossman JC, Cote M, Louie SG, Cohen ML. *Chem Phys Lett* 1998;284:344–9.